ILASS-Americas 22nd Annual Conference on Liquid Atomization and Spray Systems, Cincinnati, OH, May 2010

A Computational Study of Viscoelastic Droplet Collisions

Kyle Mooney, Sandeep Menon, and David P. Schmidt*
Department of Mechanical and Industrial Engineering
University of Massachusetts, Amherst, MA 01003

Abstract

A computational study of oblique binary viscoelastic droplet collisions is performed. The free surface is modeled by a Lagrangian moving-mesh interface tracking method which is validated against analytical solutions and experimental data for binary Newtonian droplet collisions. Interpolation error due to cell deformation is minimized with a local topological mesh adaptation algorithm. This method was then applied to the collision of viscoelastic droplets through a finite volume implementation of the linearized Phan-Thien-Tanner constitutive stress model. The extensional nature of an oblique droplet collision highlights the effects of the large Trouton ratios typically found in this class of fluids though increased stabilization of fluid ligament structures and expansion of the coalsence regime. By altering the spray kinematics in this manner, the spray characteristics as a whole are altered by the viscoelastic rheological effects. The fully three dimensional computational study investigated the effect of Weber number, and impact parameter on collision outcomes of viscoelastic droplets.

*Corresponding Author: schmidt@ecs.umass.edu

Introduction

Atomizing sprays are encountered regularly in many industrial applications including inkjets, coatings, and combustion. The coalescence and separation modes of the atomized colliding droplets can greatly affect downstream spray kinematics due to changes in size and velocity distributions [1]. Difficulties arise when experimentally quantifying this phenomenon, even with dense spray diagnostics, due to the wide range of time and length scales inherent in an atomization process. Numerical simulations can shed light into the nature of binary droplet collisions as well as complement sub-grid spray models.

Binary collisions of Newtonian droplets have been studied extensively in experimental settings. One of the earliest works on the topic by Ashgriz and Poo [2] precisely determined collision outcome regimes of water droplets using relevent dimentionless groups. Qian and Law [3] continued in a similar manner with a study of hydrocarbon droplet collisions in ambient nitrogen producing a series of high resolution time resolved photographs. These images have since become a common benchmarking tool for many CFD packages that involve free surface or interfacial physics simulation. Additionaly, viscosity has been shown by Willis [4] and Dai [5] to affect the maximum deformation of the binary system. Through experimentation, Motizigemba et al. [6] found that the time to reach maximum deformation of a shear-thinning droplet pair was independant of viscosity characteristics but the magnitude of that deformation was not. Additionally, they showed through simulation that elongational velocity gradients generally dominate shear gradients for $\chi = 0$ collision systems. In theory this elongational flow dominance could manifest itself in fluids with strain dependant Troutan ratios.

The work by G. S. de Paulo et al. [7] successfully coupled the marker and cell (MAC) interface tracking method to PTT viscoelastic rheology and were able to simulate both jet buckling and extrudate die swell. In the field of droplet collisions Yue [8] modeled coalescence and retraction of two dimensional viscoelastic droplets using the Oldroyd-B stress model but the range of Weber and Reynolds numbers explored were lower than those typically encountered in an atomizing spray [9] which is part of the novelty of this study.

Methodology

This computational study solved the incompressible Cauchy equation of momentum conservation on a cell centered finite volume mesh. Conservation of momentum, Eqn.1 was solved on moving, deforming control volumes.

$$\rho(\frac{\partial \mathbf{u}}{\partial t} + \nabla \cdot \phi \mathbf{u}) = -\nabla p + \nabla \cdot \boldsymbol{\sigma} \tag{1}$$

The variable ϕ is the volumetric flux, $\mathbf{u}$ is velocity, and p is the pressure, all defined at cell faces. ρ is the density and $\boldsymbol{\sigma}$ represents the deviatoric stress tensor before application of a constituative stress model. In this work there are two stress models employed to solve for a stress tensor $\boldsymbol{\tau}$: classical Newtonian and the Phan-Thien-Tanner viscoelastic model. For Newtonian cases $\boldsymbol{\tau}$ is defined as

$$\boldsymbol{\tau} = \mu[\nabla \mathbf{u} + (\nabla \mathbf{u})^{\mathrm{T}}] \tag{2}$$

where μ is the dynamic Newtonian viscosity of the fluid. Among the models compiled in the viscoelastic CFD library by J. Fávero [10] (the library used in this study) is the Phan-Phien-Tanner consituative stress model by Tanner [11] which is of the form:

$$f(tr(\boldsymbol{\tau}))\boldsymbol{\tau} + \lambda \overset{\nabla}{\boldsymbol{\tau}} = 2\eta \mathbf{D} \tag{3}$$

The symbol $\overset{\nabla}{(.)}$ represents the upper-convected derivative and λ is the stress relaxation time of the fluid. $\overset{\nabla}{\boldsymbol{\tau}}$ is then defined as

$$\overset{\nabla}{\boldsymbol{\tau}} = \frac{D\boldsymbol{\tau}}{Dt} - \boldsymbol{\tau} \cdot \mathbf{L} - \mathbf{L}^T \cdot \boldsymbol{\tau} \tag{4}$$

$\mathbf{L}$ represents the effective velocity gradient

$$\mathbf{L} = \Delta \mathbf{u} - \zeta \mathbf{D} \tag{5}$$

where ζ is a shear modifier which represents relative slip of polymer chains. $\mathbf{D}$ is the symmetric rate of deformation tensor

$$\mathbf{D} = \frac{1}{2}(\nabla \mathbf{u} + (\nabla \mathbf{u})^T) \tag{6}$$

The stress coeffecient is

$$f(tr(\boldsymbol{\tau})) = 1 + \frac{\lambda \varepsilon}{\mu_p} tr(\boldsymbol{\tau}) \tag{7}$$

where ϵ is an effective extensional viscosity modifier and used along with ζ as a fitting parameter. The effective polymer viscosity is μ_p and $tr()$ is the tensor trace operator. Because $f(tr(\boldsymbol{\tau}))$ is linear with respect to $\boldsymbol{\tau}$, this particular formulation is more commonly known as the linear Phan Thien Tanner (LPPT) model.

Due to the inherent numerical instability of the high Deborah number simulations being considered, the both-sides-diffusion (BSD) [12] technique is used. This makes the assumption that

the fluid is comprised of two rheologically distinct components: a viscoelastic-polymeric solute and a Newtonian solvent with independant viscosities μ_p and μ_s respectively. Additional diffusion terms are then added to both sides of the momentum equation as shown in Eqn.8 which greatly improves numerical stabiliy.

$$\rho(\frac{\partial \mathbf{u}}{\partial t} + \nabla \cdot \phi\mathbf{u}) - (\mu_s + \mu_p)\nabla^2\mathbf{u} = -\nabla p + \nabla \cdot \boldsymbol{\tau} - \mu_p \nabla^2 \mathbf{u} \quad (8)$$

This is the final form of the momentum equation used in simulation.

While many previous numerical studies of droplet collisions employ the interace capturing volume of fluids method (VOF), this paper uses an explicit interface tracking method by Dai et al. [13]. In this approach, the free surface corresponds to a (tesselated) surface of zero thickness, as opposed to interface-capturing Eulerian techniques, where the interface is of finite thickness with smoothly varying properties. A particularly attractive feature of this interface capturing approach is the precise description of interface curvature, which allows surface tension calculations to be performed with a high degree of accuracy and ensures mass conservation up to machine accuracy.

The jump in surface force $\Delta\mathbf{f}$ across an immiscible fluid interface between fluids 1 and 2 as presented by Pozrikidis [14] is

$$\Delta\mathbf{f} = \mathbf{f}^{(1)} - \mathbf{f}^{(2)} = (\boldsymbol{\sigma}^{(1)} - \boldsymbol{\sigma}^{(2)}) \cdot \mathbf{n} \quad (9)$$

where $\mathbf{n}$ is the unit normal pointing into fluid 1. In this singe phase simulation the interface is modeled shear free such that

$$\mathbf{f}^{(2)} = \boldsymbol{\sigma}^{(2)} = \boldsymbol{\sigma}^{(1)} \cdot (\mathbf{I} - \mathbf{nn}) = 0 \quad (10)$$

where $\mathbf{I}$ is the identity tensor and $\boldsymbol{\sigma}^{(1)} \cdot (\mathbf{I} - \mathbf{nn})$ represents the shear components of the stress tensor. From Tukovic [15], the free surface normal stress balance in vector form is

$$p\mathbf{n} - \mathbf{n} \cdot \boldsymbol{\sigma} = \sigma\kappa\mathbf{n} + \nabla_s\sigma \quad (11)$$

where $\nabla_s\sigma$ represents the surface divergence of the interfacial surface tension and κ is twice the mean curvature calculated by $\kappa = -\nabla_s \cdot \mathbf{n}$. Interfacial displacement is modeled in a Lagrangian fashion using the free surface evolution algorithm proposed by Muzaferija and Peric [16] which uses a coupled node and control surface scheme. The overall code stucture uses the Open Source Field Operations and Manipulations (OpenFOAM) CFD library by Weller and Jasak [17].

Throughout the literature, the Weber number ($We = \rho U^2 R/\sigma$), Reynolds number ($Re = 2\rho RU/\mu$), and impact parameter (χ) are considered the primary dimentionless groups in a study of collision outcome regimes where U is the relative droplet velocity and R is the droplet radius. With the addition of a viscoelastic dimentionless group, the Deborah number ($De = \lambda U/R$), to the typical droplet collision parameters illustrated in Fig.1, a large three dimentional parameter space is created. As this is a preliminary investigation into viscoelastic rheological effects on collision outcomes, parametric data generation will be limited to the plane $De = 70$.

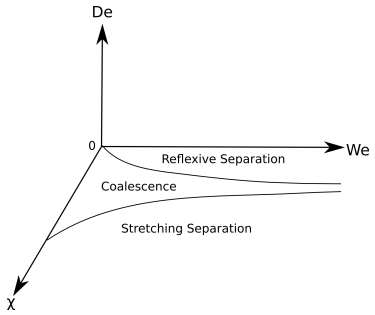

Figure 1: Representative viscoelastic collision outcome parameter space with the plane $De = 0$ representing a Newtonian fluid.

Initial free surface coalescence was assumed at the onset of simulation and implemented by joining the drops in a preprocessing step with a small mesh "bridge". This mesh connection creates a single free surface as shown in Fig.2. The ratio of drop diameter to initial bridge diameter is 0.16 for the cases investigated.

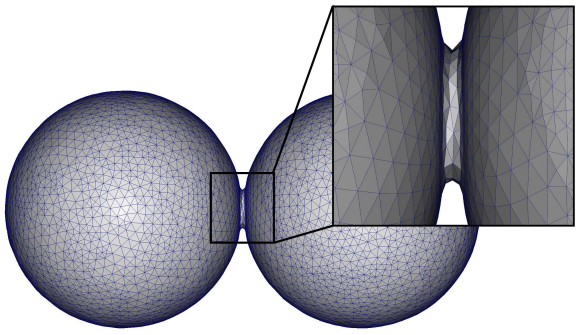

Figure 2: Illustration of mesh connection used to unify drops prior to simulation start.

$\frac{\sigma}{\rho}(m^3/s^2)$	1e-5	1e-6	1e-7
T(s): Theoretical value	0.022214	0.070248	0.22214
T(s): Test value	0.022412	0.070886	0.22617
Percent Error	0.89%	0.91%	1.81%

Table 1: Results for oscillating droplet validation test

Numerical Validation

The accuracy of the free surface treatment was validated via the simulation of a spherical mode-2 oscillating droplet. Analytical solutions to the oscillation period T and viscous decay time constant t_c were derived from perturbation analysis by Lamb [18]. The drop was given an initial purturbation such that ratio of the major and minor axes lengths of the oblate spheriod was 1.03 corresponding to a 3 percent perturbation. The case was performed without need of topological adaption algorithms as the surface purturbation was subtle enough that interior cell distortion was within tolerance. Oscillation period was calculated by

$$T = 2\pi \frac{1}{\sqrt{8\frac{\sigma}{\rho r_0^3}}} \tag{12}$$

where r_0 is the droplet's radius at spherical equilibrium. The droplet was modeled with 50,184 tetrahedral cell volumes. Results in Table.1 show strong analytical agreement for various $\frac{\sigma}{\rho}$ ratios. The viscous dissipation rate was validated using the time constant equation

$$t_c = \frac{\rho r_0^2}{(n-1)(2n+1)\eta} \tag{13}$$

where n is the mode of oscillation, in this case, 2. Simulated results are shown in Fig.3 and are in agreement with analyical results. The further validate the free surface algorithms, benchmark experiments performed by Qian and Law [3] were reproduced in the simulation environment. Good qualitative agreement is shown in Fig.4.

There exists an analytical solution to the deviatoric stress and velocity profiles of a PTT fluid in pressure driven channel flow derived by Olivera and Pinho [19]. Following a similar validation as G. S. de Paulo et al. [7], these solutions are used to verify implementation of the LPPT model. Case assumptions include no slip velocity conditions at both walls and a channel center line at $y = 0$. A pressure gradient ∇p is perscribed along the flow direction. Analytical velocity and stress profiles are shown to be in excellent agreement with simulation results as shown in Fig.5

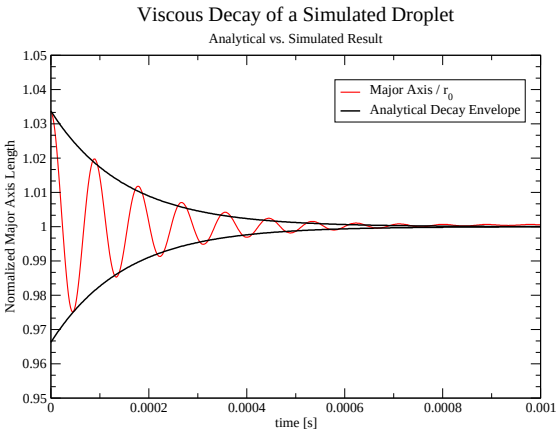

Figure 3: Viscous decay envelope of a simulation droplet.

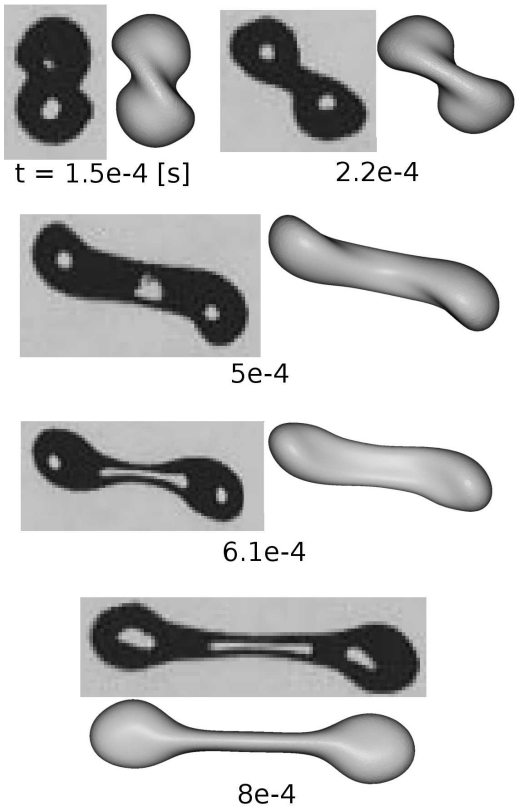

Figure 4: Qualitative time paired comparison of experimental run "o" from Qian and Law [3] and simulation result. $We = 60.8, Re = 313.7, \chi = 0.68$.

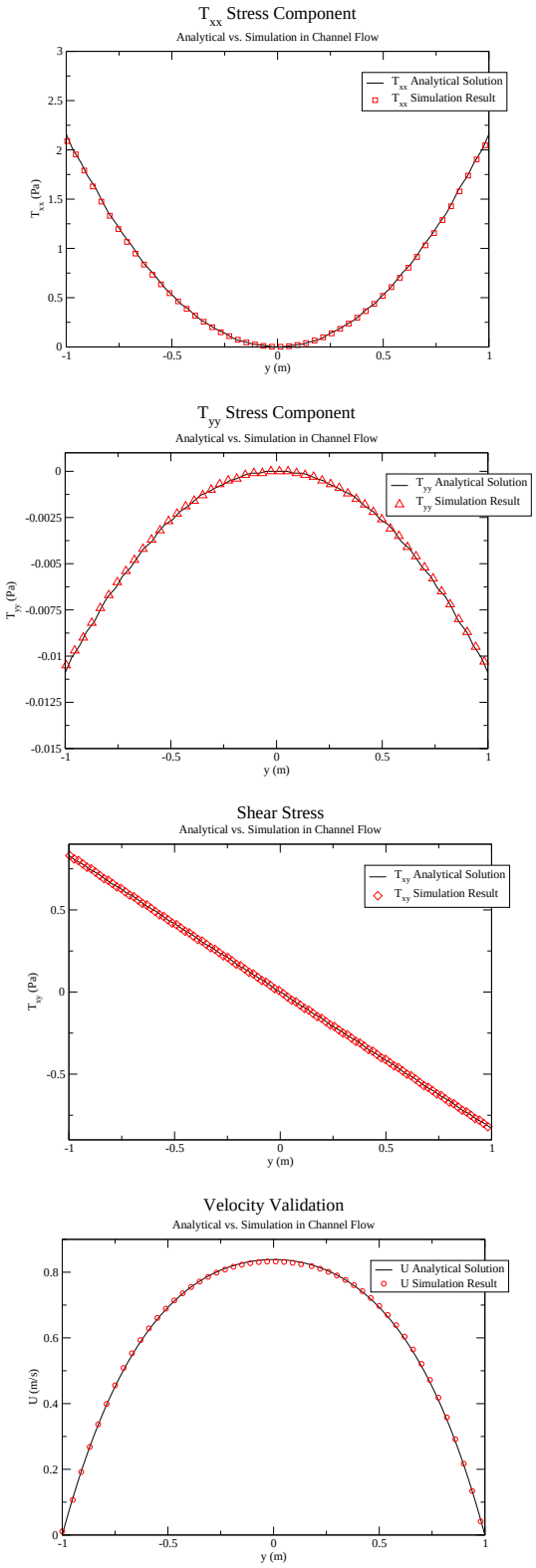

Figure 5: Comparison of simulated PTT fluid in channel flow against the analytical solution.

Preliminary Results

Collision results thus far show an expaned coalescence regime as shown in Fig.6. Here, Newtonian outcome regime boundaries are marked in black lines. The coalescence-stretching separation boundary for a PTT fluid with $De = 70$ is predicted to lie within the blue dotted lines. Further sampling will yield a more precise predicted boundary zone which will be published in a future work.

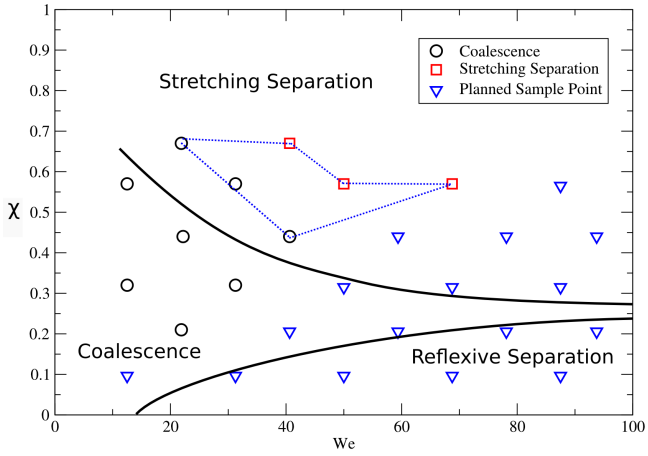

Figure 6: Overlay of a Newtonain collision map and viscoelastic droplet collision results.

Conclusions

A widened coalescence zone could be expected from a PTT fluid due to the extensional thickening behavior of the model. Examples of simulated coalesence and stretching separation are show in Fig.7 and Fig.8 repectively. The differences shown thus far between the Newtonain and viscoelastic collision maps illustrate the need for specifically viscoelastic spray models.

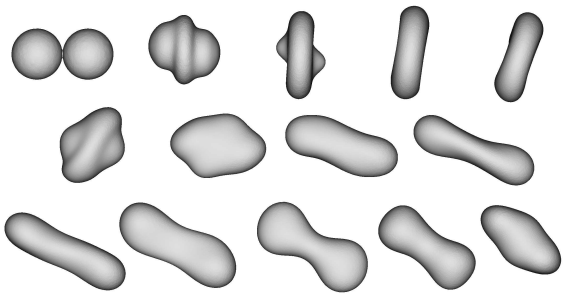

Figure 7: Simulated viscoelastic drop coalescence. $(We = 21.88, \chi = 0.21, De = 70)$

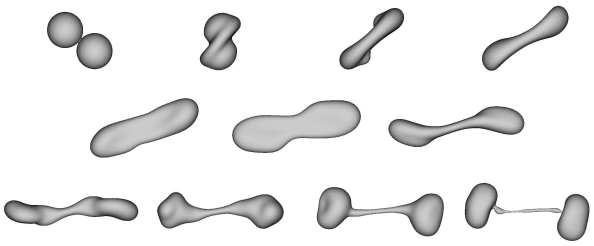

Figure 8: Simulated stretching separation of viscoelastic droplets. ($We = 50, \chi = 0.565, De = 70$)

Acknowledgments

We acknowledge the financial support of the Army Research Office under grant number W911NF-08-1-0171. We also thank Hrvoje Jasak, Zeljko Tuković, and Jovani Favero for OpenFOAM software library contributions.

References

[1] A Theodorakakos M Gavaises and G Bergeles. *Journal of Mechanical Engineering Science*, 210(5):465–477, 1996.

[2] Ashgriz N. and Poo J.Y. *Journal of Fluid Mechanics*, 221:183–204, 1990.

[3] J. Qian and C. K. Law. *Journal of Fluid Mechanics*, 1997.

[4] K. Willis and M. Orme. *Experiments in Fluids*, 34:28–41, 2003.

[5] Meizhong Dai and David P. Schmidt. *Physics of Fluids*, 17, 2005.

[6] D. Bothe M. Motizigemba, N. Roth and H. J. Warnecke. *Fourteenth International Conference on Liquid Atomization and Spray Systems*, Zaragoza, Spain, September.

[7] M.F. Tome G.S. de Paulo and S. McKee. *Journal of Non-Newtonian Fluid Mechanics*, 147:149–174, 2007.

[8] Chun Liu Pengtau Yue, James J. Feng and Jie Shen. *Journal of Non-Newtonian Fluid Mechanics*, (129):163–176, 2005.

[9] Gunnar Stiesch. *Modeling Engine Spray and Combustion Processes*. Springer, 2003.

[10] Jovani Luiz Fávero. Simulação de escoamentos viscoelãsticos : desenvolvimento de uma metodologia de anãlise utilizando o software openfoam e equações constitutivas diferenciais. Master's thesis, Federal University of Rio Grande do Sul, 2009. In Protuguese.

[11] N. Phan-Thien and R. I. Tanner. *Journal of Non-Newtonian Fluid Mechanics*, (2):353–365, 1977.

[12] S. C. Xue R. I. Tanner and N. Phan-Thien. *Journal of Non-Newtonain Fluid Mechanics*, 2004.

[13] Meizhong Dai and David P. Schmidt. *Journal of Computational Physics*, 208(1):228–252, 2005.

[14] C. Pozrikidis. *Introduction to Theoretical and Computational Fluid Dynamics*. Oxford University Press, 1997.

[15] Z. Tuković. PhD thesis, University of Zagreb, 2005. In Croatian.

[16] S. Muzaferija and M. Peric. *Numerical Heat Transfer*, 1997.

[17] H. Jasak H. G. Weller, G. Tabor and C. Fureby. *Computers in Physics*, 12(6):620–631, 1998.

[18] H. Lamb. *Hydrodynamics*. Dover Publications Inc., 1945.

[19] Paulo J. Olivera and Fernando T. Pinho. *Journal of Fluid Mechanics*, 387:271–280, 1999.